The initial stages of multicomponent particle formation during the gas phase combustion synthesis of mixed SiO2/TiO2

Fang, Jiaxi

2018

Fang , J , Wang , Y , Kangasluoma , J , Attoui , M , Junninen , H , Kulmala , M , Petäjä , T & Biswas , P 2018 , ' The initial stages of multicomponent particle formation during the gas phase combustion synthesis of mixed SiO2/TiO2 ' , Aerosol Science and Technology , vol. 52 , no. 3 , pp. 277-286 . https://doi.org/10.1080/02786826.2017.1399197

http://hdl.handle.net/10138/306287
https://doi.org/10.1080/02786826.2017.1399197

acceptedVersion

The initial stages of multicomponent particle formation during the gas phase combustion synthesis of mixed SiO_2/TiO_2

Jiaxi Fang[1,#], Yang Wang[1,#,*], Juha Kangasluoma[2], Michel Attoui[2,3], Heikki Junninen[2], Markku Kulmala[2], Tuukka Petäjä[2], and Pratim Biswas[1*]

[1]Aerosol and Air Quality Research Laboratory
Department of Energy, Environmental and Chemical Engineering
Washington University in St. Louis
St. Louis, MO-63130

[2] Department of Physical Sciences,
University of Helsinki, P.O. Box 64, Helsinki, 00014, Finland

[3] LISA Université paris Est, Diderot, Créteil, 7583, France

Revised manuscript submitted to:

Aerosol Science and Technology

October 24, 2017

# These authors contributed equally to this work.

* To whom correspondence should be addressed:

Pratim Biswas: Tel: +1-314-935-5548; Fax: +1-314-935-5464; E-mail: pbiswas@wustl.edu
Yang Wang: Tel: +631-344-8138; Fax: +1-631-344-2887; E-mail: yangwang@bnl.gov

Change of address: the current address of Yang Wang is

Environmental & Climate Sciences Department, Brookhaven National Laboratory, Bldg. 815E, PO Box 5000, Upton, NY 11973

Abstract

The ability to properly scale the synthesis of advanced materials through combustion synthesis routes is limited by our lack of knowledge regarding the initial stages of particle formation. In flame aerosol reactors, the high temperatures, fast reaction rates, and flame chemistry can all play a critical role in determining the properties of the resulting nanomaterials. In particular, multicomponent systems pose a unique challenge as most studies rely on empirical approaches towards designing advanced composite materials. The lack of predictive capabilities can be attributed to a lack of data on particle inception and growth below 2 nm. Measurements for the initial stages of particle formation during the combustion synthesis of SiO_2 and composite SiO_2/TiO_2 using an atmospheric pressure inlet time-of-flight mass spectrometer are presented. Both positively and negatively charged clusters can be measured and results show the presence of silicic acid species which grow through dehydration, hydrogen abstraction, and interactions with hydroxyl radicals. In the case of composite SiO_2/TiO_2 particle formation, new molecular species containing Ti atoms emerge. Tandem differential mobility analysis-mass spectrometry (DMA-MS) provided further insight into the size-resolved chemistry of particle formation to reveal that at each cluster size, further hydroxyl driven reactions take place. From this we can conclude that previous assumptions on collisional growth from simple monomer species of SiO_2 and TiO_2 does not sufficiently describe the collisional growth mechanisms for particle growth below 2 nm.

1. Introduction

Combustion synthesis is a versatile technique for producing advanced nanomaterials such as alumina, silica, titania, and other metal oxides (Li et al. 2016). At industrial scales, utilization of combustion synthesis poses the advantages of large production rates, high purity, and low waste generation. More specifically, silica and titania nanoparticles synthesized through this route have found applications for use as hydrophobic coatings, pigments, and catalysts. The successful application of this technology requires an adequate degree of tailoring and control in regards to nanoparticle properties which often requires doping. Doping during combustion synthesis has been limited in scalability due to difficulties in preventing phase segregation and controlling material properties such as crystal structure and particle size. A more detailed understanding of particle formation pathways, beginning with the initial stages, for composite nanoparticles synthesized via combustion synthesis will be critical in the successful application of this technology.

TiO_2 and SiO_2 are two major products from flame synthesis due to the low cost of synthesis precursors and their wide applications in catalysis, solar energy utilization, sensor technology, and paint production (Kammler et al., 2001; Liu et al., 2015). By properly mixing these two oxides, the products are found to possess enhanced catalytic and optical performances in certain applications (Fu et al., 1996; Strobel et al., 2006; Tricoli et al., 2009). Previous studies on doped systems have been able to successfully synthesize composite silica-titania nanomaterials. For example, Ehrman et al. (1999) examined the properties of binary TiO_2 /SiO_2 systems while carefully studying the conditions for phase segregation. In addition, the prevention of phase segregation could be achieved by carefully controlling the downstream conditions of the flame

through dilution quenching (Teleki et al. 2005). More advanced nanostructures of TiO_2 nanoparticles have been able to add coatings of silica (Teleki et al. 2005), noble metal decorations (Tiwari et al. 2008) and doping with copper (Sahu et al. 2011). With proper control, the addition of dopants can result in enhanced performance for catalysis (Thimsen et al. 2009) and energy conversion (Hu et al. 2017). Challenges for achieving scalability for these applications include the ability to control new nanoparticle formation in flame aerosol reactors. This stems from a lack of understanding for the initial stages of particle formation (Carbone et al. 2016; Fang et al. 2014; Tang et al. 2017; Wang et al. 2014; Wang 2017). Despite the significant effort placed on properly designing doped nanomaterials, successful industrial production is limited by a lack of predictive capabilities for modeling flame aerosol reactors for scale up.

Titania and silica particle formation mechanisms have been studied independently using the precursors of titanium tetraisopropoxide (TTIP) and tetraethyl orthosilicate (TEOS). These precursors are commonly used to for the combustion synthesis of nanoparticles. Conversion from precursor molecules to oxide monomers is often assumed to be simplified global mechanisms such as thermal decomposition or hydrolysis (Tsantilis et al. 2002; Wang et al. 2015). Under classical nucleation theory, the critical particle size for a stable oxide seed particle is below the mass-based particle diameter of a single oxide molecule. Thus, studies have assumed that the critical nucleus for a stable monomer is a single oxide molecule, while further growth is assumed to occur through collisions of these monomers. Recently, theoretical modeling has yielded more detailed pathways of TEOS decomposition to silica, and have demonstrated the importance of intermediate species towards the conversion of TEOS to SiO_2. Such intermediate are formed through de-methylation, de-ethylation, demethylation and disproportionation, and de-ethylation

and dehydration pathways (Phadungsukanan et al. 2009). Similar studies have examined TTIP decomposition using statistical thermodynamics, quantum chemistry, and equilibrium composition analysis which agree with experimental results (Shmakov et al. 2013). Although recent work has mapped out such pathways in detail, there is a lack of experimental validation at the molecular level for cluster growth.

The goal of this study is to measure cluster formation mechanisms for multicomponent systems of TiO_2 and SiO_2 in a flame aerosol reactor. The chemistry of decomposition for both precursors has been well studied thus providing a good basis for understanding the initial stages of mixed oxide particle formation. Previous studies have mainly focused on conversion mechanism from precursors to stable monomers but did not consider how these byproducts may interact with one another to grow into stable nanoparticles. By using an atmospheric pressure interface time-of-flight (APi-TOF) mass spectrometer, natively charged clusters are measured to infer their chemical composition and track their growth mechanisms.

2. Material and Methods

2.1. Experimental setup

Single component SiO_2 and multicomponent SiO_2/TiO_2 clusters were generated using a premixed methane air flat flame aerosol reactor (Wang et al. 2017a; b). Figure 1 displays the experimental setup where methane (CH_4, >99.95%, Linde AG), oxygen (O_2, >99.95%, Linde AG), nitrogen carrier gas (N_2, >99.95%, Linde AG), and gaseous precursor were premixed and stabilized over a 1.91 cm diameter flat flame burner head. A stream of N_2 with a flow rate of 3 lpm was also provided with a concentric outer tube of 2.54 cm to shield the flame from

entraining excess air. Tetraethyl orthosilicate (TEOS, >97%, Sigma Aldrich) and titanium (IV) isopropoxide (TTIP, >97%, Sigma Aldrich) precursors were delivered using a glass sealed bubbler (MDC Vacuum Products, LLC) while N_2 was used as the carrier gas. All gas flow rates were controlled by mass flow controllers (MKS Instruments). Precursor loading rates were calculated using vapor pressure data available for TTIP (Siefering and Griffin 1990) and TEOS (Jang 1999). In this study, the TEOS precursor feed rate was maintained at 0.44 mmol/hr (17.6 ppm). During the synthesis of TiO_2/SiO_2 particles, the molecular ratio of Ti/Si was controlled at 0.5. Details on flow conditions are provided in Table 1.

The initial stages of nanoparticle formation during combustion synthesis were measured by an atmospheric-pressure interface time-of-flight (APi-TOF) mass-spectrometer (TOFwerk AG, Thun, Junninen et al. (2010)). Flame generated clusters were sampled using a venturi dilution probe (5 mm above the head of the burner) to rapidly quench further collisional growth and chemical reactions. The gas dilution ratio was 180:1 with a dilution flow of 25 lpm. Excess flow was exhausted while a portion of the diluted sample was directly injected into the entrance of the APi-TOF mass spectrometer with an inlet flow rate of 0.81 slpm regulated by a critical orifice at the instrument inlet. Only natively charged clusters were measured and no additional ionization was added to the system. The atmospheric pressure interface (APi) guided the sampled ions from the atmospheric pressure to the TOF while pumping away the gas. Existing measurements conducted with an ultrafine particle counter indicated that the charged fraction of incipient particles during combustion could be extremely high due to intense chemical ionization (Wang et al. 2017a). Hence, the APi-TOF measured charged clusters could represent the properties of the nascent particles generated during combustion synthesis. The APi-TOF had a resolution of 3000

Th/Th (M/ΔM) with a mass accuracy of 20 ppm and a detection range of up to 2500 Th. Before measurements, the mass accuracy of the APi-TOF was calibrated with acetone or nitrate ions generated by feeding gas vapors through a radioactive neutralizer (Fang et al. 2017). Mass spectra was analyzed using a MATLAB program previously developed for high resolution mass spectrometers (Junninen et al. 2010). The confirmation of probable molecular compositions was based on both the highly accurate mass and isotope distributions. However, due to isotope peak overlap and the multiple combinations of potential compounds at high mass ranges, exact peak assignments could not be performed at large m/z values (>450 Th), thus mass defect techniques were used to provide further insight into the mass spectra. The particle loss in the system took place predominantly in the APi-TOF, which was reported to have a transmission efficiency of 0.1 to 0.5% (Junninen et al. 2010). The compositions of the detected clusters are strongly affected by the ions generated from combustion, since charging and coagulation took place simultaneously during the particle formation. Therefore, changes made to flames that will alter the ion generation will inevitably change the composition and further affect the mobility of the detected clusters (Fialkov, 1997). A previous study (Wang et al., 2017c) showed that the mobility distributions of flame-generated ions are influenced by the flame equivalence ratio and the sampling height of the dilution probe. Dilution ratio also affects the mobility distribution of the clusters; however, it was found that the normalized mobility distribution remained the same after the dilution ratio increased beyond 133 (Fig. S1). The influence of precursor feed rates on cluster composition was found to be small, as indicated by the unchanged chemical composition and effective densities of the clusters during the synthesis of SiO_2 (Wang et al., 2017b).

2.2. Size-resolved chemistry with differential mobility analysis-mass spectrometry (DMA-MS)

The size-resolved particle chemical composition could provide more information about particle formation and growth in the initial stages. In addition to the mass analysis, high-resolution differential mobility analysis was implemented to obtain particle size distributions (Hogan Jr and de la Mora 2009; Maißer et al. 2015), which was done by adding a Herrmann-type differential mobility analyzer (DMA) upstream of the APi-TOF, as shown in Fig. 1. The Herrmann-type DMA allows for the classification of clusters based on their electrical mobility (Z) ranging from 0.1-7.5 Vs/cm^2 (Kangasluoma et al. 2016). A closed loop configuration for the DMA was used to maintain a balanced flow rate of 10.81 lpm for the inlet and outlet of the DMA. Recirculating room air was used initially while the flow rate for the DMA was maintained by an inline DC brushless blower (DOMEL Inc.) operated with a flow rate above 500 lpm. However, due to the closed-loop configuration, the DMA was quickly saturated with nitrogen provided by the dilution sampling probe. The particle mobility was obtained through calibration by electrospraying a mobility standard of tetraheptylammonium bromide (99.9%, Sigma-Aldrich) diluted in methanol (Ude and Fernandez de la Mora 2005). In order to remove any excess nanoparticles and contaminants, an in line HEPA filter was added to the recirculating sheath flow. The mobility spectra were obtained by scanning the DMA voltage using a high voltage source (Spellman Inc.) which was controlled using LabView with a voltage step of 3V and a 1s step time. After mobility classification, one stream of particles was introduced to a faraday-cage electrometer (EM, Model 3068B, TSI Inc.) to be measured with concentration, and another stream of particles was injected to the inlet of the APi-TOF, which measured the molecular mass for the classified particles. The particle mobility size was further calculated using the Stokes-Cunningham-Millikan equation (Tammet 1995) $Z = Cne/3\pi\mu D_p$, where Z is the measured particle mobility, C is the Cunningham slip correction factor, n is the number of charges on the

particle, e is the electronic charge, μ is the air viscosity, and D_p is the particle mobility size. The particle size distributions have also been measured by a scanning mobility particle sizer (SMPS) composed of a Nano DMA (Model 3085, TSI Inc.) and a condensation particle counter (Model 3776, TSI Inc.). Due to the low precursor feed rate, particles above 3 nm could not be detected by the SMPS setup.

2.3. Experimental plan

The experimental plan is presented in Table 2 for examining multicomponent cluster formation mechanisms. Test 1 will measure the mass spectra for natively charged single component SiO_2 clusters by adding a TEOS precursor into the FLAR. Test 2 will examine multicomponent systems with the addition of both TTIP and TEOS precursor for TiO_2/SiO_2 nanoparticle synthesis. Finally, test 3 will examine the size-resolved chemistry of cluster formation during the initial stages of nanoparticle formation with tandem DMA-MS.

3. Results and discussion

3.1. Single component particle growth mechanisms.

Molecular species of natively charged clusters generated during the combustion synthesis of SiO_2 were measured in an APi-TOF Mass spectrometer. Measuring natively charged clusters allows for the direct observation of new particle formation during combustion synthesis. Figure 2 shows representative mass spectra for both positively and negatively charged clusters from the particle formation of SiO_2. Si species could be identified based upon three naturally occurring isotopes: $^{27.9769}$Si (92.2%), $^{28.9765}$Si (4.6%), and $^{29.9738}$Si (3.1%). By examining the charged cluster mass and their isotope patterns, we can begin to study new particle inception and how

these particles grow beyond monomeric species. There are noticeable difference in spectra patters for positively (Fig. 2a) and negatively charged (Fig. 2b) clusters. Certain peaks could be identified and their proposed molecular compositions and molecular weights are listed in Table S1.

In the case of positively charged clusters, the highest intensity peaks in the positive mass spectra are protonated silicic acid ($Si(OH)_4H^+$, 96.9957 Th), protonated TEOS monomers ($Si(OC_2H_5)_4H^+$, 209.1204 Th), and protonated TEOS dimers ($(Si(OC_2H_5)_4)_2H^+$, 417.2340 Th). The high signal intensity suggested that these three compounds were more stable in the flame. The detected high concentrations of $Si(OH)_4$ is in agreement with previous studies, where $Si(OH)_4$ is the main product of TEOS decomposition and is the most stable product of TEOS decomposition in the temperature range of 800-2200 K based on thermodynamic equilibrium calculations (Phadungsukanan et al. 2009). Positively charged clusters are proposed to be formed through the protonation of silicates from collisions with hydronium ions and hydroxyl radicals in the flame. The presence of TEOS monomers and dimers implies incomplete decomposition of precursor molecules, thus further decomposition is expected to take place downstream leading to potential surface growth mechanisms. In addition, intermediate hydrocarbon species from TEOS decomposition were detected in lower concentrations in the form of ethoxy and methoxy silanes including $Si(OCH_2)(OC_2H_5)_3$, $Si(OH)_2(OC_2H_5)_2$, and $Si(OCH_3)_2(OC_2H_5)_2$. These species have been previously established as important intermediates in the decomposition of TEOS through various pathways such as ethylene elimination and radical additions (Nurkowski et al. 2015).

The representative mass spectra for negatively charged species from Fig. 2b yielded a wider variety of silicate peaks throughout the mass spectra. Most of the negatively charged silicate ions were in the form of $Si_nO_x(OH)_y$ with an attached nitrate ion or nitric acid cluster, where the size of a cluster, n, represents the number of Si atoms within the oxide complex. The attachment of nitrate ions and nitric acid clusters to most of the negatively charged clusters demonstrates the presence of chemical ionization in the flame (Wang et al. 2017c). The formation of negatively charged species is hypothesized to form through charge exchange and proton transfer between nitrate ions and silicate species. It might also be possible that the attachment of nitrate species was completed in the sampling system, where the rapid cooling altered the equilibrium of reactions. However, the obtained knowledge can be applied to molecular doping and the synthesis of quantum dots during combustion, where rapid dilution is needed in these scenarios. The high concentration of silicic acid clusters agrees well with previous theoretical studies which have hypothesized particle growth to begin with a $Si(OH)_4$ seed particle with successive growth occurring through $Si(OH)_4$ addition and dehydration reaction pathways (Shekar et al. 2012).

From Fig. 2a and Table S1, various silicate monomer species were measured, thus demonstrating the possibility that additional hydrogen abstraction and oxidation reactions are taking place in the flame. Various monomers may participate in cluster growth, which begins with the formation of dimers through hydrogen abstraction and collisional growth of $SiO(OH)_3$ and dehydration reactions from $Si(OH)_4$ to form Si-O-Si ligands. Furthermore, collisions between monomers and dimers will yield trimers of silicic acid species with hydroxyl groups attached with siloxane bond linking Si atoms. Clusters with up to 5 Si atoms could be identified, and proceeded to have similar collisional growth pathways through the formation of siloxane bonds. Beyond 450 Th,

the molecular composition of peaks could not be assigned due to the high number of possible compounds and drift in calibration. Nonetheless, here we have presented the first measurements for the formation pathways of silicic acid clusters during combustion synthesis of SiO_2.

3.2. Multicomponent new particle formation

The next step towards understanding composite nanoparticle formation was to add TTIP TEOS precursor to the flame aerosol reactor to study TiO_2/SiO_2 composite particle formation. The intent is to study whether SiO_2 clusters and TiO_2 clusters form independently from each other or initially interact to form mixed oxides. For comparison, Table S1 includes representative Ti-containing clusters measured during the premixed flame synthesis of TiO_2 by a recent study (Fang et al., 2017) and the spectrum of these Ti-containing clusters are shown in Figs. S2 and S3. Figure 3 displays the mass spectra for the resulting negatively charged clusters with the single component spectra and multicomponent spectra plotted together. Many of the peaks for the multicomponent mass spectra overlap with those of the single component mass spectra, showing that products from pure SiO_2 particle formation are still present. Based on the distinct isotopic pattern of Ti atoms ($^{45.9526}$Ti (10.8%), $^{46.9518}$Ti (9.9%), $^{47.9480}$Ti (73.8%), $^{48.9479}$Ti (7.5%), $^{49.9448}$Ti (7.3%)), we can easily distinguish between Ti- and Si-containing species. The emergence of new peaks can also be seen beginning with an integer m/z of 236 Th. At this mass, two possible species exist: $TiO_4(NO_3)^-$ (235.903 Th), and $Si_2O(OH)_6NO_3^-$ (235.954 Th). However, the distinct isotope pattern of a Ti-containing cluster indicates the presence of titanium at this peak. Furthermore, larger Ti-containing molecules with various Ti:O ratios could be identified such as $TiO_2(NO_3)_3^-$ (265.901 Th) and $Ti_3(OH)_{11}^-$(330.874 Th). In the earlier stages of particle inception, each component will form smaller clusters independently. This supports previous work which

has studied the growth of iron oxide-silica nanocomposites in flames (Biswas et al. 1997; McMillin et al. 1996). These studies concluded that particle nucleation begins independently for each component. For larger cluster masses beyond 400 Th in Fig. 3, previously prominent Si peaks are less prominent, providing evidence for the formation of multicomponent clusters due to the inevitable collisional growth between Si and Ti clusters. These results suggested that the smaller clusters were predominantly generated via combustion process and the larger clusters were likely to be formed above the reaction zone of the flame via a heterogeneous process. In multicomponent systems, the decomposition of precursors and formation of clusters most likely occurs independently, however beyond a critical cluster size, composite clusters will form beyond cluster sizes of 5. In larger m/z ranges, however, we cannot identify the exact molecular composition of these species due to limitations in resolution and complexity of the spectra from overlapping isotope peaks. Under this situation, the mass defect plot may provide more information on multicomponent particle formation in the early stages.

The mass defect of a molecular species is the difference between the accurate molecular mass and nominal (integer) molecular mass. A mass defect plot shows the relationship between the accurate molecular mass and mass defect of the APi-TOF detected molecular clusters. Owing to the isotope distributions certain elements, the mass defect plot could better distinguish species with different chemical compositions. Using mass defect plots, recent work showed that the clusters generated during the early stages of TiO_2 formation can be categorized to different bands with specific number of Ti atoms, while CH_2 abstraction was the major reaction during TTIP thermal decomposition during combustion (Fang et al. 2017). Figure 4 shows the mass defect plots of positively charged particles generated during the formation of SiO_2 and TiO_2/SiO_2

composite particles. The mass defect plot of particles generated during the formation of SiO_2 can be divided into two regions (Fig. 4a): 100 to 500 Th where the mass defect increases with molecular mass, and beyond 500 Th where the mass defect decreases with molecular mass. The increase of mass defect was mainly caused by the existence of hydrogen ($^{1.0078}$H) in the molecular species. Therefore, the clusters detected below 500 Th were mainly associated with precursor molecules and indicated the occurrence of precursor reactions. Above 500 Th, the mass defects decreased, which is caused by the addition of silicon ($^{27.9769}$Si (92.2%), $^{28.9765}$Si (4.6%), and $^{29.9738}$Si (3.1%)) and oxygen ($^{15.9949}$O), since both elements have negative mass defects. Furthermore, the slope of the decreasing mass defect also matches with that of pure SiO_2 clusters (-0.055 Th/100 Th). Hence, the decrease of mass defect demonstrates the formation of SiO_2 particles. It should be noted that the mass defect plot obtained during SiO_2 formation distinguished significantly that of TiO_2 formation (Fig. 4b), where clear bands of Ti-containing clusters could be observed. This difference could be attribute to the different chemical properties TTIP and TEOS. When both precursors were added to the flame, new patterns of the mass defects emerged starting from 350 Th (Fig. 4c). This new pattern differs from that obtained from either SiO_2 or TiO_2 formation, which confirms the cluster interaction and the formation of composite nanoparticles.

3.3. Tandem DMA-MS

In order to gain more insight into the size-resolved chemistry of new particle formation, tandem DMA-MS was used to measure the mass of ions with respect to their electrical mobility (mobility size). Although high-resolution DMAs are very effective at classifying charged clusters based on their mobility size, electrical mobility alone is not sufficient for characterizing the

initial stages of particle formation, since it cannot provide information on the chemical formation pathway of nanoparticles. Using tandem DMA-MS can overcome these limitations while further providing insight into the size-resolved chemistry for clusters below 2 nm. Figure S4 displays a resulting mobility scan for ions as measured by a high-resolution DMA for both single component and multicomponent cases (Ti/Si=0.5). For the synthesis of pure SiO_2, several distinct ion peaks can be observed ranging from 0.46 Vs/cm^2 to 0.81 Vs/cm^2 (mobility diameter of 0.99-1.31 nm). In the case of multicomponent TiO_2/SiO_2 nanoparticle formation, the peaks shifted to the right indicating the formation of larger clusters and monomer scavenging. This is also confirmed by the higher concentration of particles with sizes larger than 2 nm, which is beyond the scale of Fig. S4.

The composition of the classified charged particles at each mobility were measured by maintaining a fixed voltage across the DMA at each peak from the mobility distribution (Fig. S4), collecting the mass spectra using the APi-TOF mass spectrometer. Figure 5 displays resulting mass spectra at fixed electrical mobilities where a series of ions classified by their electrical mobility. The mass spectra of multiple species were measured under a single mobility set by the DMA, which is mainly caused by the lower resolution of the DMA compared to the TOF mass spectrometer. Although the Herrmann DMA is a high-resolution DMA, the theoretical resolution of the Herrmann DMA under the flow rate settings used in this study was approximately 20 to 30 (Kangalsuoma et al., 2016), while the APi-TOF has a resolution of 3000. This difference in resolution would result in multiple species detected by the APi-TOF under a single mobility of set by the DMA. On the other hand, the mobility of the cluster below 2 nm is strongly affected by its shape and chemical composition. Clusters with different mass values may

possess very similar mobility values. For each growing cluster size (increasing inverse mobility), multiple stable molecular species are present with various degrees of oxidation. For example, cluster sizes with 4 Si atoms are measured at an electrical mobility of 0.71 Vs/cm^2, where 4 stable species including $Si_4(OH)_7$, $Si_4(OH)_8O_4$, $Si_4O_3(OH)_{10}$, and $Si_4O(OH)_8$ can be detected at this electrical mobility. From the presence of these species, we can see that adjacent hydroxyl sites may react to reduce the oxidation state of Si towards the steady state form of SiO_2. Previous attempts to model cluster growth have assumed that for each discrete size, a uniform molecular composition exists. These results show that for the growth of oxide nanoparticles, significant reactions such as hydrogen abstraction and dehydration reactions can occur even within a discrete cluster size. Most likely, due interactions with attached hydroxyl groups, hydrogen abstraction and dehydration are occurring within cluster sizes.

Similarly, for multicomponent systems, DMA-MS revealed the presence of multiple ion peaks at a fixed electrical mobility (Fig. 6). The first peak, measured at 0.49 Vs/cm^2 was not displayed as it was a single cluster of HNO_3NO_3. At the subsequent peaks, species of Ti monomers emerge at both 0.56 Vs/cm^2 and 0.59 Vs/cm^2. Three main peaks at 236 Th, 248 Th, and 265 Th emerge at different intensities and could be identified as oxidized Ti monomers with nitrate radicals attached. For the first two peaks at 0.56 Vs/cm^2 and 0.59 Vs/cm^2, due to the lower resolving power, the DMA was unable to completely resolve the monomer Ti peaks at 236 and 265 Th. At higher inverse mobilities, previously detected Si peaks are less prominent in high concentrations, most likely due to scavenging.

The relationship between mass and mobility in the free molecular regime is not well understood and can depend significantly on material properties. Figure 7 maps the measured mass to charge as a function of the inverse mobility from tandem DMA-MS measurements. A dashed line in the plot indicates the Kilpatrick relationship (Kilpatrick 1971), which is a commonly utilized relationship for estimating cluster mass with respect to electrical mobility in this size range. Clearly all the measured clusters are well above the Kilpatrick relationship, indicating that clusters of Si and Ti are much denser. Larriba et al. (2011) have proposed molecular modeling approaches to predict this relationship and highlighted the limitation of the Kilpatrick relationship. However, there are no simulations for composite and doped nanoparticles available in the literature to compare against the data produced in this study. By converting the measured mobility diameters to volumetric diameters using the relationship proposed by Larriba et al. (2011), the effective densities of the detected clusters could be calculated using the similar method provided by Wang et al. (2017b). The particles generated from flames with the addition of TEOS and mixed TEOS and TTIP had effective densities of 1.42g/cm^3 1.57 g/cm^3. The effective density of the clusters formed during multicomponent particle synthesis is in between the values reported by Wang et al. (2017b) for single component SiO_2 and TiO_2 synthesis (1.42 and 1.75 g/cm^3), suggesting the formation of clusters with mixed compositions. Studies relying on high-resolution DMAs in this size range should have a clearer understanding of the measured ions chemical composition.

4. Conclusions

This work presents the first measurements of the new particle formation during the combustion synthesis of silica and composite silica/titania clusters. Using an atmospheric pressure inlet time-

of-flight mass spectrometer (APi-TOF), the cluster growth mechanisms, starting from monomers, for positively and negatively charged species in a flame are studied. Cluster growth mechanisms can be seen for silica, as collisional growth between small clusters yield the presence of silicic acid units linked by siloxane bonds. The addition of TTIP precursor results in scavenging of silicate species to form larger clusters. By applying tandem DMA-MS, we examined the size-resolved chemistry of cluster growth mechanisms. Results indicate significant chemistry occurring between clusters, since silicate species of various Si:O ratio were present at the same Si cluster size. In the case of multicomponent systems, Ti-containing species appear to dominate the mass spectra as Si species can no longer be measured in high concentrations indicating the possible formation of mixed clusters.

Acknowledgements

This work is supported by the Solar Energy Research Institute for India and the United States (SERIIUS), funded jointly by the U.S. Department of Energy (Office of Science, Office of Basic Energy Sciences, and Energy Efficiency and Renewable Energy, Solar Energy Technology Program, under Subcontract DE-AC36-08GO28308 to the National Renewable Energy Laboratory, Golden, Colorado) and the Government of India, through the Department of Science and Technology under Subcontract IUSSTF/JCERDC-SERIIUS/2012. The work was also supported by Academy of Finland via Center of Excellence project in Atmospheric Sciences (272041) and European Commission via ACTRIS2 (654109).

References

Biswas, P., Wu, C. Y., Zachariah, M. R., McMillin, B. (1997). Characterization of iron oxide-silica nanocomposites in flames: Part II. Comparison of discrete-sectional model predictions to experimental data. J. Mater. Res. 12:714-723.

Carbone, F., Attoui, M., Gomez, A. (2016). Challenges of measuring nascent soot in flames as evidenced by high-resolution differential mobility analysis. Aerosol Sci. Technol. 50:740-757.

Ehrman, S. H., Friedlander, S. K., Zachariah, M. R. (1999). Phase segregation in binary SiO_2/TiO_2 and SiO_2/Fe_2O_3 nanoparticle aerosols formed in a premixed flame. J. Mater. Res. 14:4551-4561.

Fang, J., Wang, Y., Attoui, M., Chadha, T. S., Ray, J. R., Wang, W.-N., Jun, Y.-S., Biswas, P. (2014). Measurement of sub-2 nm clusters of pristine and composite metal oxides during nanomaterial synthesis in flame aerosol reactors. Anal. Chem. 86:7523-7529.

Fang, J., Wang, Y., Kangasluoma, J., Attoui, M., Junninen, H., Kulmala, M., Petäjä, T., Biswas, P. (2017). Cluster formation mechanisms of titanium dioxide during combustion synthesis: Observation with an APi-TOF. Aerosol Sci. Technol. 50(9): 1071-1081.

Fialkov, A. B. (1997). Investigations on ions in flames. Prog. Energy Combus. Sci. 23:399-528.

Fu, X., Clark, L. A., Yang, Q., Anderson, M. A. (1996). Enhanced photocatalytic performance of titania-based binary metal oxides: TiO_2/SiO_2 and TiO_2/ZrO_2. Environ. Sci. Technol. 30:647-653.

Hogan Jr, C. J. and de la Mora, J. F. (2009). Tandem ion mobility-mass spectrometry (IMS-MS) study of ion evaporation from ionic liquid-acetonitrile nanodrops. Phys. Chem. Chem. Phys. 11:8079-8090.

Hu, Y., Jiang, H., Li, Y., Wang, B., Zhang, L., Li, C., Wang, Y., Cohen, T., Jiang, Y., Biswas, P. (2017). Engineering the outermost layers of TiO_2 nanoparticles using in situ Mg doping in a flame aerosol reactor. AIChE J. 63:870-880.

Jang, H. D. (1999). Generation of silica nanoparticles from tetraethylorthosilicate (TEOS) vapor in a diffusion flame. Aerosol Sci. Technol 30:477-488.

Junninen, H., Ehn, M., Petäjä, T., Luosujärvi, L., Kotiaho, T., Kostiainen, R., Rohner, U., Gonin, M., Fuhrer, K., Kulmala, M. (2010). A high-resolution mass spectrometer to measure atmospheric ion composition. Atmos. Meas. Tech. 3:1039-1053.

Kammler, H. K., Mädler, L., Pratsinis, S. E. (2001). Flame synthesis of nanoparticles. Chem. Eng. Technol. 24:583-596.

Kangasluoma, J., Attoui, M., Korhonen, F., Ahonen, L., Siivola, E., Petäjä, T. (2016). Characterization of a Herrmann-type high-resolution differential mobility analyzer. Aerosol Sci. Technol. 50:222-229.

Kilpatrick, W. (1971). An experimental mass-mobility relation for ions in air at atmospheric pressure, in Proc. Annu. Conf. Mass Spectrosc. 19th, 320-325.

Larriba, C., Hogan Jr, C. J., Attoui, M., Borrajo, R., Garcia, J. F., de la Mora, J. F. (2011). The mobility–volume relationship below 3.0 nm examined by tandem mobility–mass measurement. Aerosol Sci. Technol. 45:453-467.

Li, S., Ren, Y., Biswas, P., Stephen, D. T. (2016). Flame aerosol synthesis of nanostructured materials and functional devices: Processing, modeling, and diagnostics. Prog. Energy Combust. Sci. 55:1-59.

Liu, P., Arnold, I. J., Wang, Y., Yu, Y., Fang, J., Biswas, P., & Chakrabarty, R. K. (2015). Synthesis of titanium dioxide aerosol gels in a buoyancy-opposed flame reactor. Aerosol Sci. Technol., 49(12), 1232-1241.

Maißer, A., Thomas, J. M., Larriba-Andaluz, C., He, S., Hogan, C. J. (2015). The mass–mobility distributions of ions produced by a Po-210 source in air. J. Aerosol Sci. 90:36-50.

McMillin, B. K., Biswas, P., Zachariah, M. R. (1996). In situ characterization of vapor phase growth of iron oxide-silica nanocomposites: Part I. 2-D planar laser-induced fluorescence and Mie imaging. J. Mater. Res. 11:1552-1561.

Nurkowski, D., Buerger, P., Akroyd, J., Kraft, M. (2015). A detailed kinetic study of the thermal decomposition of tetraethoxysilane. Proc. Combust. Inst. 35:2291-2298.

Phadungsukanan, W., Shekar, S., Shirley, R., Sander, M., West, R. H., Kraft, M. (2009). First-principles thermochemistry for silicon species in the decomposition of tetraethoxysilane. J. Phys. Chem. A 113:9041-9049.

Sahu, M., Suttiponparnit, K., Suvachittanont, S., Charinpanitkul, T., Biswas, P. (2011). Characterization of doped TiO 2 nanoparticle dispersions. Chem. Eng. Sci. 66:3482-3490.

Strobel, R., Baiker, A., Pratsinis, S. E. (2006). Aerosol flame synthesis of catalysts. Adv. Powder Technol. 17:457-480.

Shekar, S., Sander, M., Riehl, R. C., Smith, A. J., Braumann, A., Kraft, M. (2012). Modelling the flame synthesis of silica nanoparticles from tetraethoxysilane. Chem. Eng. Sci. 70:54-66.

Shmakov, A., Korobeinichev, O., Knyazkov, D., Paletsky, A., Maksutov, R., Gerasimov, I., Bolshova, T., Kiselev, V., Gritsan, N. (2013). Combustion chemistry of Ti(OC3H7)4 in premixed flat burner-stabilized H2/O2/Ar flame at 1atm. Proc. Combust. Inst. 34:1143-1149.

Siefering, K. and Griffin, G. (1990). Growth kinetics of CVD TiO_2: influence of carrier gas. J. Electrochem. Soc. 137:1206-1208.

Tammet (1995). Size and mobility of nanometer particles, clusters and ions. J. Aerosol Sci. 26(3): 459-475.

Tang, Q., Cai, R., You, X., Jiang, J. (2017). Nascent soot particle size distributions down to 1nm from a laminar premixed burner-stabilized stagnation ethylene flame. Proceedings of the Combustion Institute 36:993-1000.

Teleki, A., Pratsinis, S., Wegner, K., Jossen, R., Krumeich, F. (2005). Flame-coating of titania particles with silica. J. Mater. Res. 20:1336-1347.

Thimsen, E., Biswas, S., Lo, C. S., Biswas, P. (2009). Predicting the band structure of mixed transition metal oxides: theory and experiment. J. Phys. Chem. C 113:2014-2021.

Tiwari, V., Jiang, J., Sethi, V., Biswas, P. (2008). One-step synthesis of noble metal–titanium dioxide nanocomposites in a flame aerosol reactor. Appl. Catal., A 345:241-246.

Tricoli, A., Righettoni, M., Pratsinis, S. E. (2009). Anti-fogging nanofibrous SiO_2 and nanostructured SiO_2–TiO_2 films made by rapid flame deposition and in situ annealing. Langmuir 25:12578-12584.

Tsantilis, S., Kammler, H., Pratsinis, S. (2002). Population balance modeling of flame synthesis of titania nanoparticles. Chem. Eng. Sci. 57:2139-2156.

Ude, S. and Fernandez de la Mora, J. (2005). Molecular monodisperse mobility and mass standards from electrosprays of tetra-alkyl ammonium halides. J. Aerosol Sci. 36:1224-1237.

Wang, Y. (2017). Sub 2 nm particle characterization in systems with aerosol formation and growth. Doctoral Dissertation. Washington University in St. Louis.

Wang, Y., Fang, J., Attoui, M., Chadha, T. S., Wang, W.-N., Biswas, P. (2014). Application of Half Mini DMA for sub 2 nm particle size distribution measurement in an electrospray and a flame aerosol reactor. J. Aerosol Sci. 71:52-64.

Wang, Y., Kangasluoma, J., Attoui, M., Fang, J., Junninen, H., Kulmala, M., Petäjä, T., Biswas, P. (2017a). The high charge fraction of flame-generated particles in the size range below 3 nm measured by enhanced particle detectors. Combust. Flame 176:72-80.

Wang, Y., Kangasluoma, J., Attoui, M., Fang, J., Junninen, H., Kulmala, M., Petäjä, T., Biswas, P. (2017b). Observation of incipient particle formation during flame synthesis by tandem differential mobility analysis-mass spectrometry (DMA-MS). Proc. Combust. Inst. 36:745-752.

Wang, Y., Liu, P., Fang, J., Wang, W.-N., Biswas, P. (2015). Kinetics of sub-2 nm TiO2 particle formation in an aerosol reactor during thermal decomposition of titanium tetraisopropoxide. J. Nanopart. Res. 17:1-13.

Wang, Y., Sharma, G., Koh, C., Kumar, V., Chakrabarty, R., Biswas, P. (2017c). Influence of flame-generated ions on the simultaneous charging and coagulation of nanoparticles during combustion. Aerosol Sci. Technol. 51:833-844.

Table Captions

Table 1. Premixed FLAR parameters

Table 2. Experimental plan more measuring multicomponent nanoparticle formation

Figure Captions

Fig. 1. Experimental setup for the combustion synthesis of SiO_2 and TiO_2 in a premixed flat flame aerosol reactor along with the measurement of charged clusters using an atmospheric-pressure-inlet time-of-flight (APi-TOF) mass spectrometer, a differential mobility analyzer (DMA), and an electrometer (EM).

Fig. 2. Natively charged clusters of measured for SiO_2 nanoparticle formation in a flame aerosol reactor for positively (A) and negatively (B) charged clusters.

Fig. 3. Direct comparison of resulting mass spectra of natively charged clusters for composite TiO_2/SiO_2 (black) and single component SiO_2 (gray) nanoparticle formation in a flame aerosol reactor.

Fig. 4. Mass defect plots of incipient positively charged particles generated during the formation of (a) SiO_2 (b) TiO_2, and (c) TiO_2/SiO_2 composite particles. s.

Fig. 5. Negative mass spectra at a fixed electrical mobility for pure SiO_2 nanoparticle synthesis.

Fig. 6. Negative mass spectra for composite TiO_2/SiO_2 nanoparticle synthesis at a fixed electrical mobility.

Fig. 7. Comparison of the mass-mobility relationship for clusters of SiO_2 and composite TiO_2 /SiO_2 clusters measured by tandem DMA-MS. The size of the circle is scaled to the peak signal intensity.

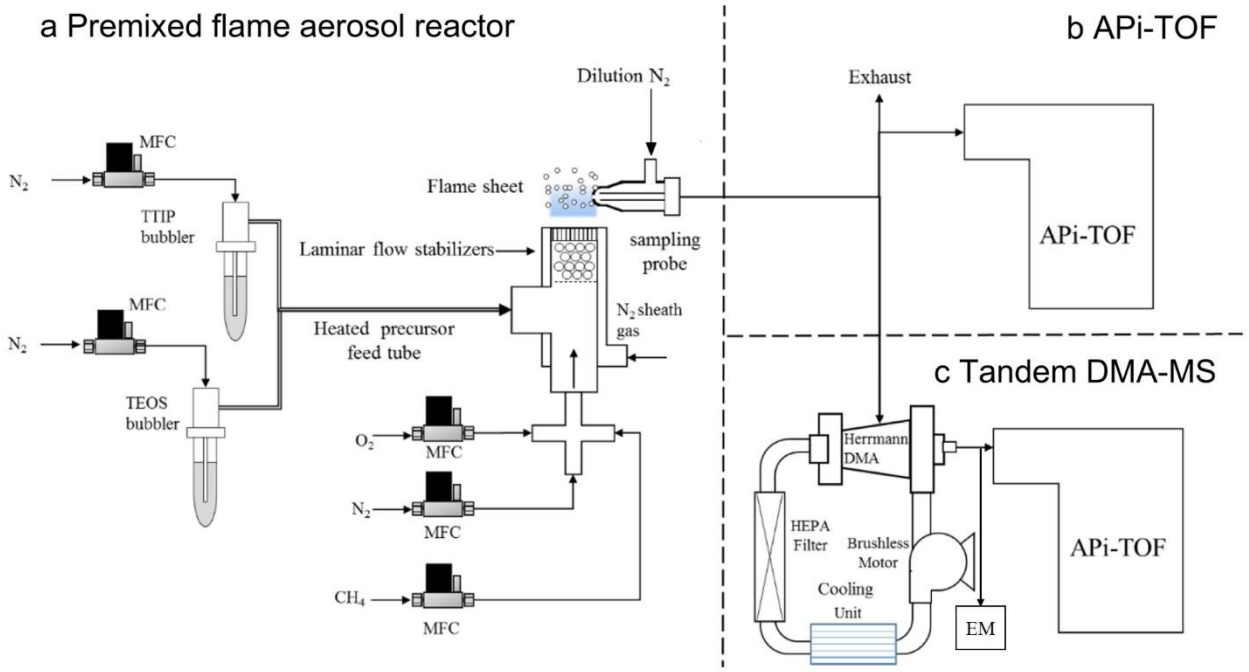

Fig. 1. Experimental setup for the combustion synthesis of SiO_2 and TiO_2 in a premixed flat flame aerosol reactor along with the measurement of charged clusters using an atmospheric-pressure-inlet time-of-flight (APi-TOF) mass spectrometer, a differential mobility analyzer (DMA), and an electrometer (EM).

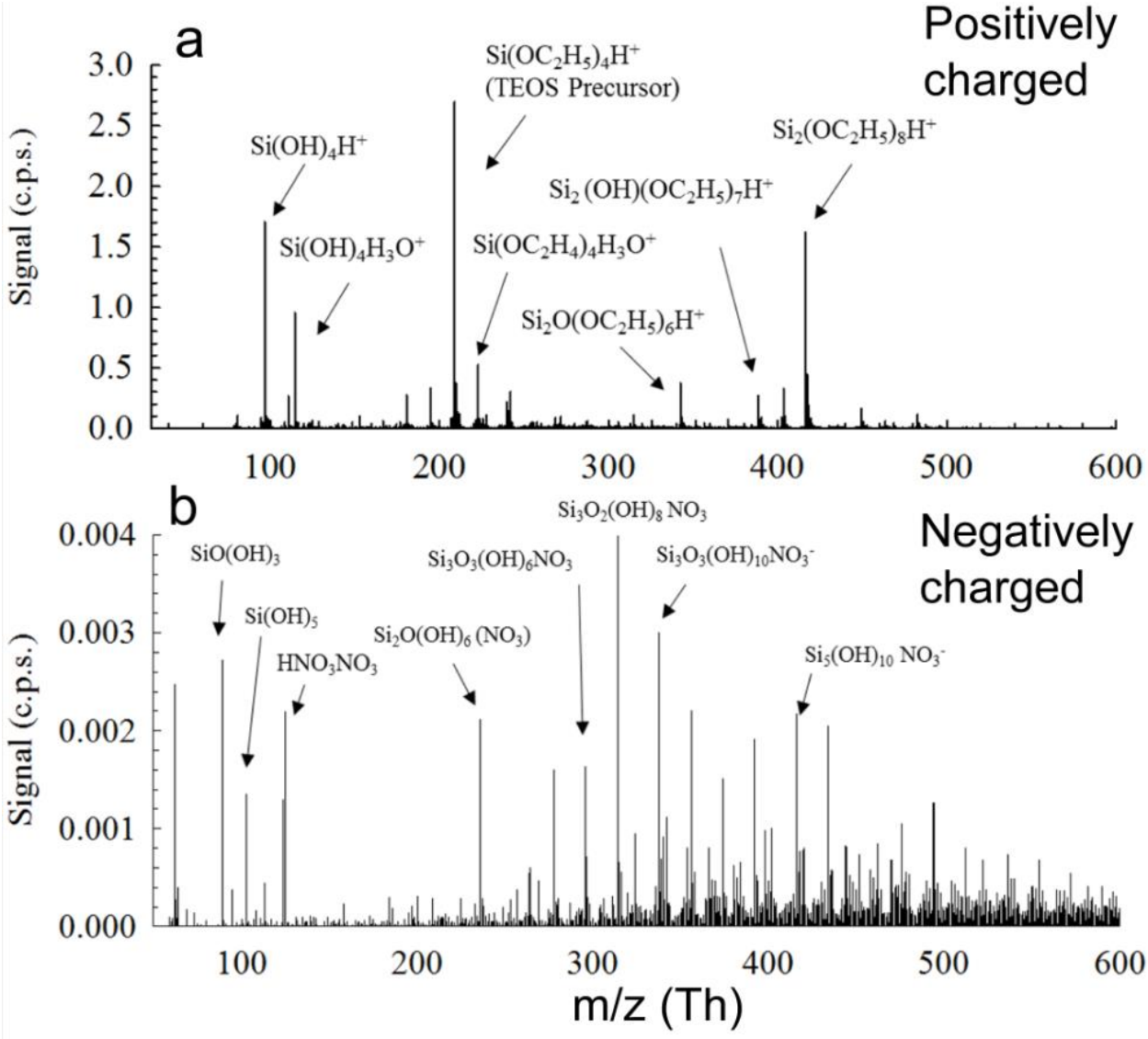

Fig. 2. Natively charged clusters of measured for SiO_2 nanoparticle formation in a flame aerosol reactor for positively (A) and negatively (B) charged clusters.

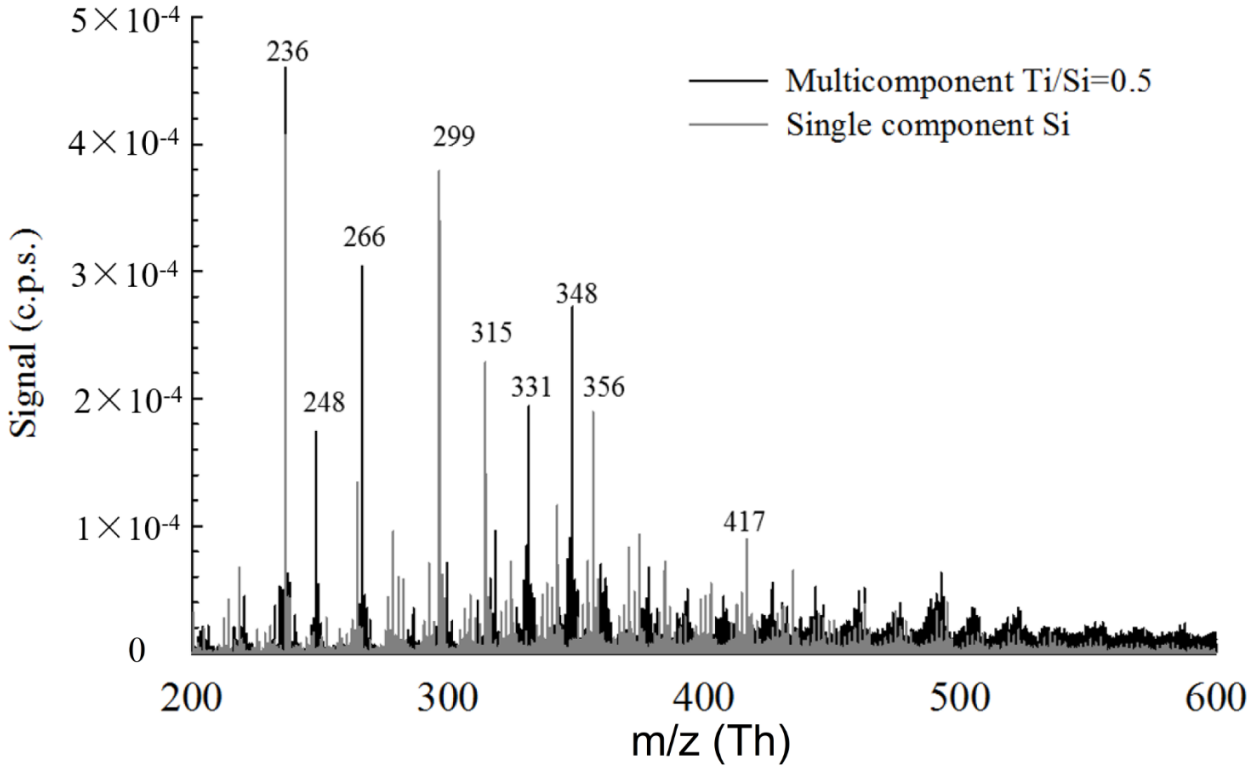

Fig. 3. Direct comparison of resulting mass spectra of natively charged clusters for composite TiO_2/SiO_2 (black) and single component SiO_2 (gray) nanoparticle formation in a flame aerosol reactor.

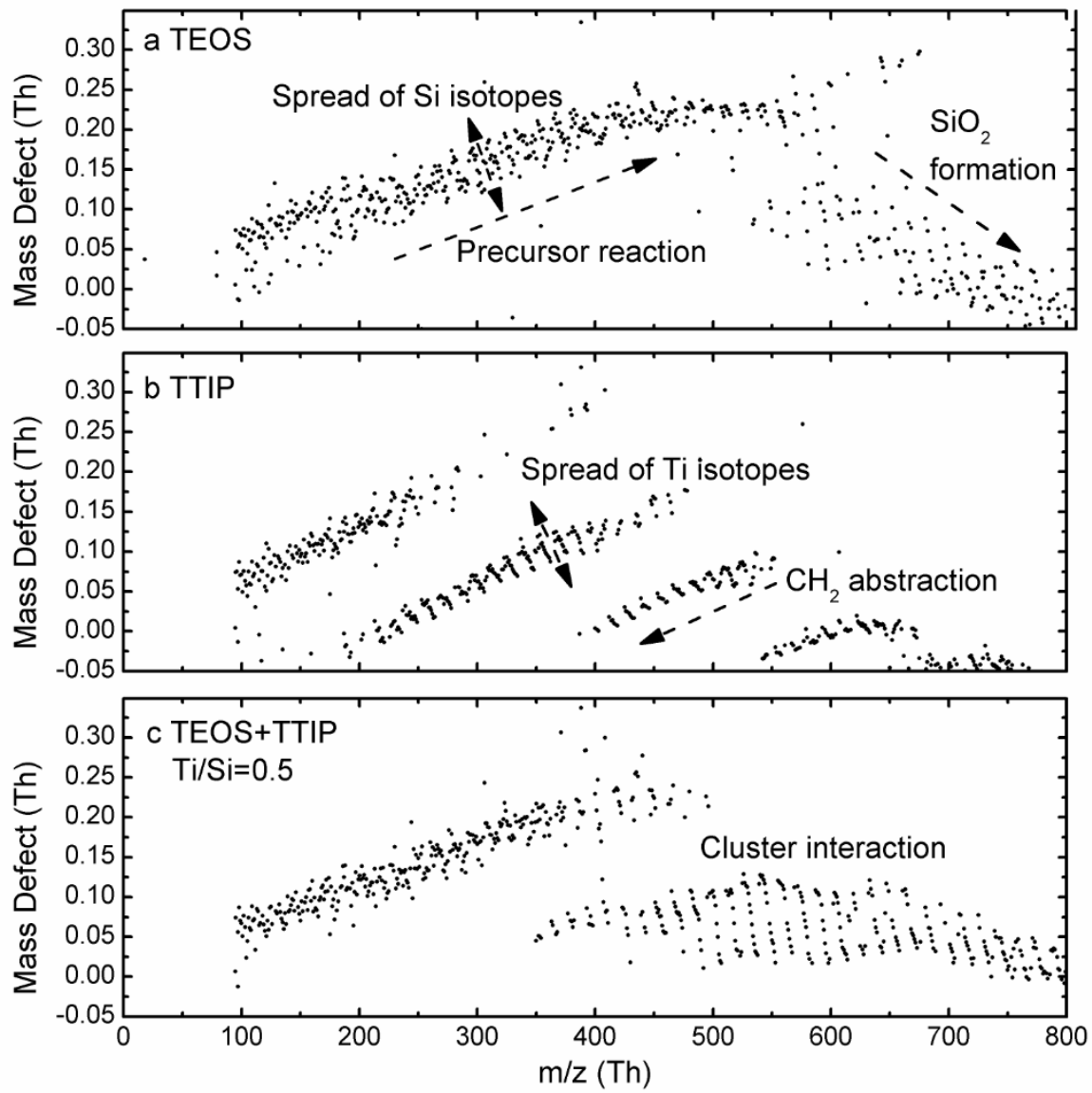

Fig. 4. Mass defect plots of incipient positively charged particles generated during the formation of (a) SiO_2 (b) TiO_2 (Fang et al., 2017), and (c) TiO_2/SiO_2 composite particles.

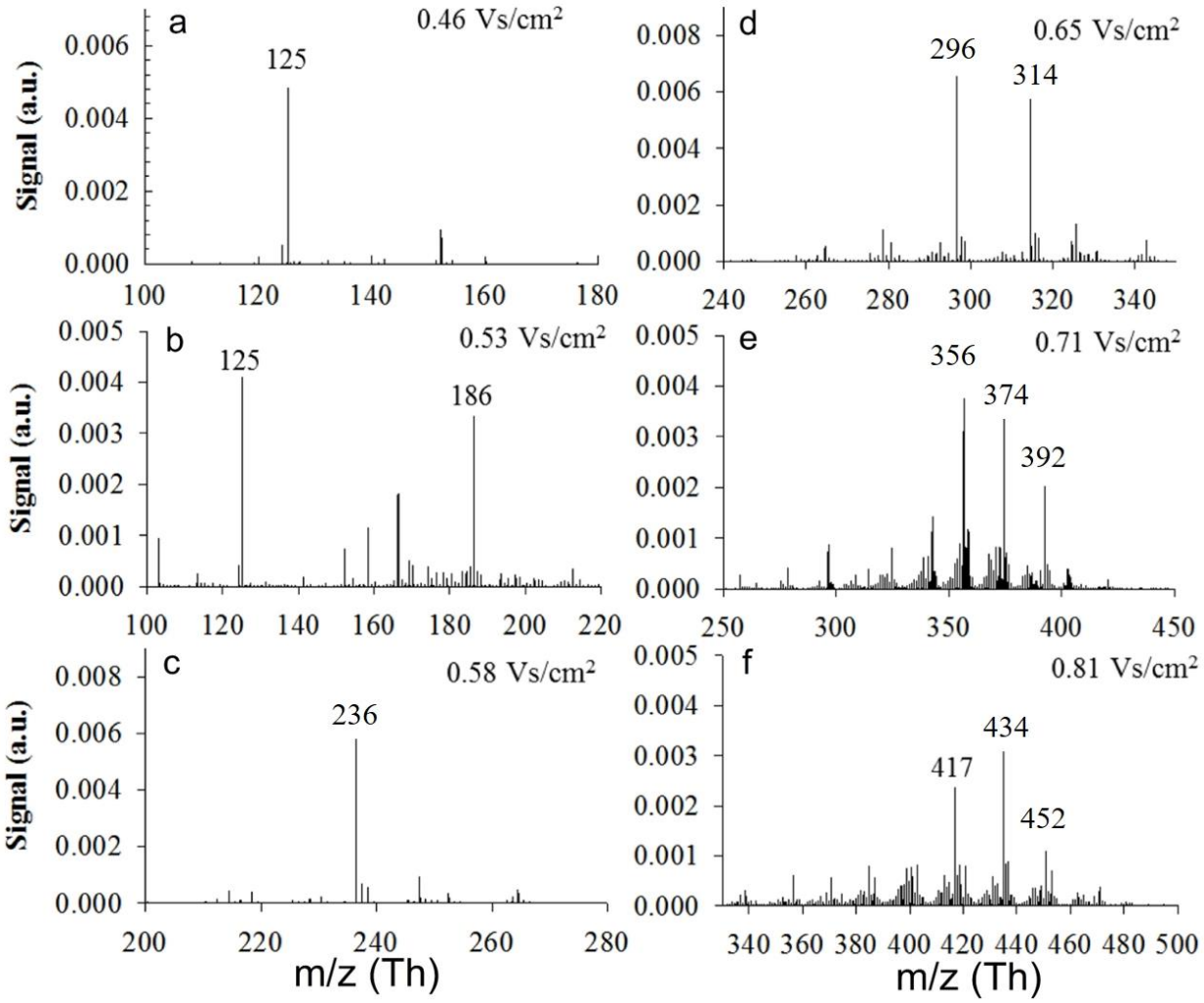

Fig. 5. Negative mass spectra at a fixed electrical mobility for pure SiO_2 nanoparticle synthesis.

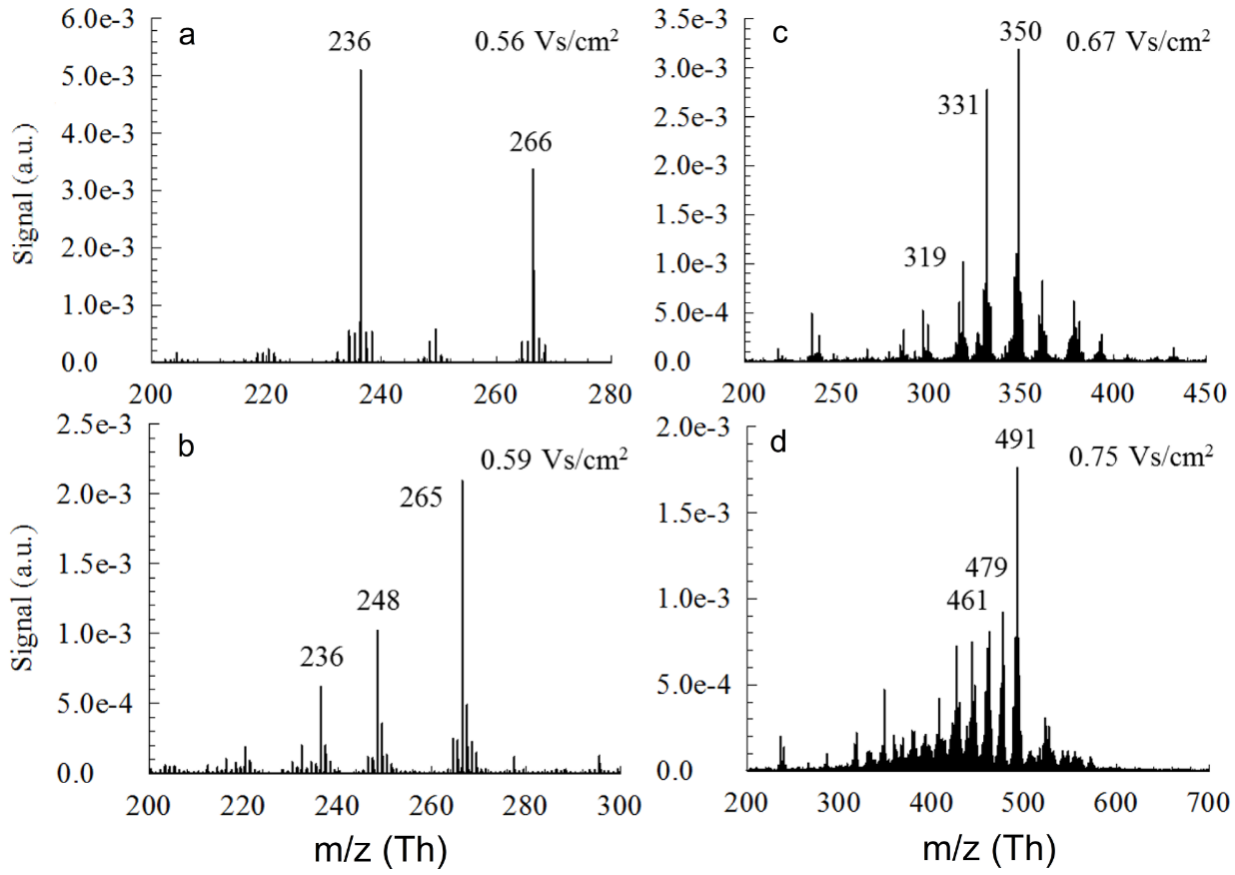

Fig. 6. Negative mass spectra for composite TiO_2/SiO_2 nanoparticle synthesis at a fixed electrical mobility.

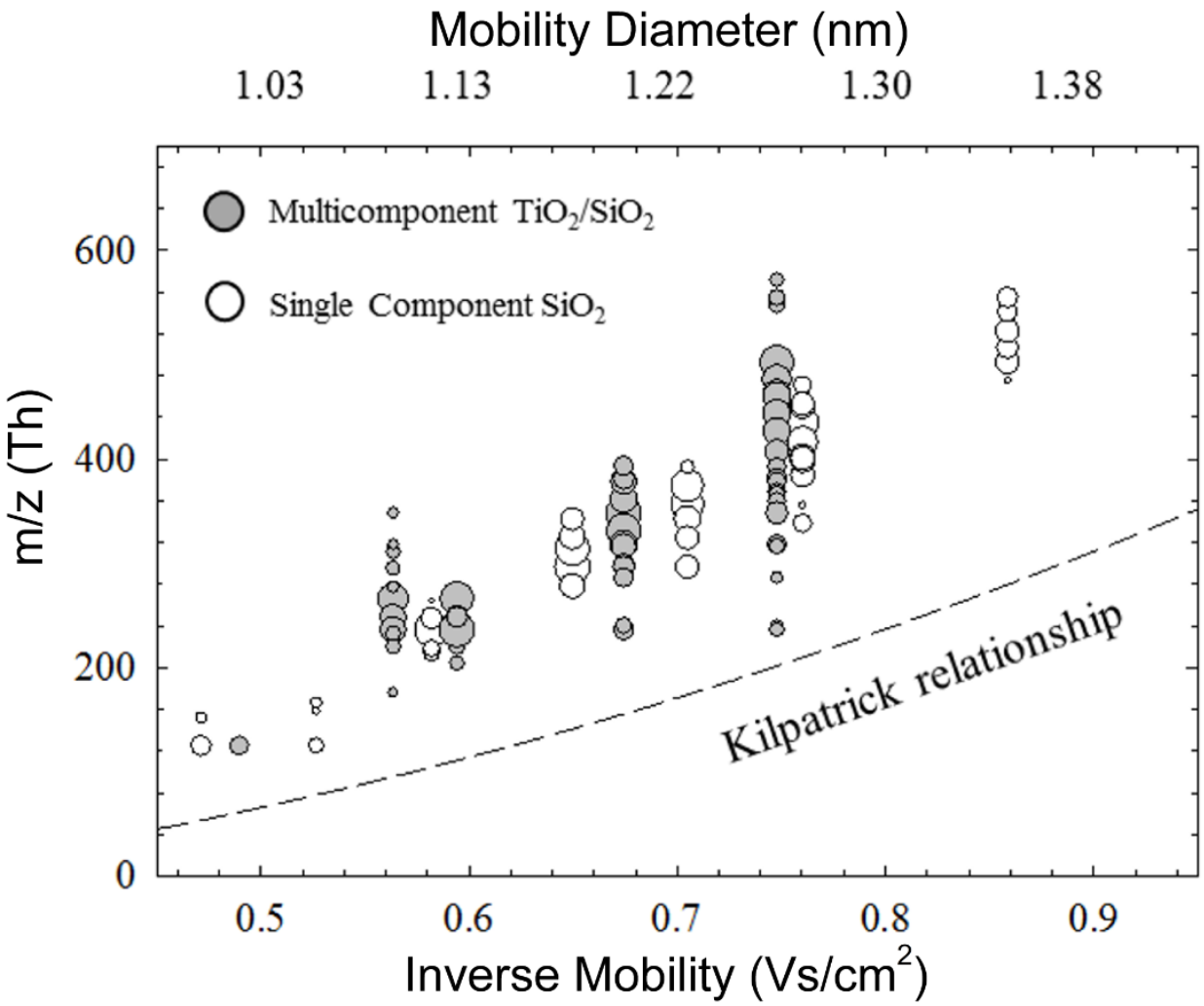

Fig. 7. Comparison of the mass-mobility relationship for clusters of SiO_2 and composite TiO_2 /SiO_2 clusters measured by tandem DMA-MS. The size of the circle is scaled to the peak signal intensity.

Table 1. Premixed flame aerosol reactor parameters and operating conditions.

Property	**Value**
Methane flow rate	1.0 lpm
Oxygen flow rate	2.85 lpm
Nitrogen flow rate	6.5 lpm
Sampling probe dilution ratio	180:1
Flame diameter	1.91 cm
TEOS precursor feed rates	0.44 mmol/hr
TTIP precursor feed rate	0/0.22 mmol/hr

Table 2. Experimental plan.

Test #	Objective	APi-TOF	DMA	TEOS	TTIP
1	Measure natively charged clusters for pure SiO_2 particle formation	✓	×	✓	×
2	Measure mixed TiO_2 /SiO_2 composite nanoparticle formation	✓	×	✓	✓
3	Examine size-resolved chemistry in a tandem DMA-MS system	✓	✓	✓	✓